Catalysis Today 151 (2010) 244–250

Contents lists available at ScienceDirect

Catalysis Today

journal homepage: www.elsevier.com/locate/cattod

High deNOx performance of Mn/TiO_2 catalyst by NH_3

Young Jin Kim[a], Hyuk Jae Kwon[a], In-Sik Nam[a,*], Jin Woo Choung[b], Jeong Ki Kil[b], Hong-Jip Kim[b], Moon-Soon Cha[c], Gwon Koo Yeo[c]

[a] Department of Chemical Engineering/School of Environmental Science and Engineering, Pohang University of Science and Technology (POSTECH), San 31 Hyojadong, Pohang 790-784, Republic of Korea
[b] Exhaust Emission Engineering Team, Power Train R&D Center, Hyundai-Kia Motors, Hwaseong 445-706, Republic of Korea
[c] Technology Center, Ordeg Corporation, Ansan 425-100, Republic of Korea

ARTICLE INFO

Article history:
Available online 18 April 2010

Keywords:
Urea-SCR
Mn/TiO_2
Sol–gel
Low temperature SCR
Fast SCR reaction

ABSTRACT

The deNOx performance of the s-Mn/TiO_2 catalyst prepared by sol–gel method has been significantly enhanced, particularly in the low temperature region. Mn is basically incorporated into the matrix of Ti and becomes a structural component of s-MnO_2/TiO_2 mixed oxide, whereas by impregnation method it simply exists on the surface of i-Mn/TiO_2. The well-dispersed Mn over s-Mn/TiO_2 catalyst is the primary cause for the high deNOx performance compared to that over i-Mn/TiO_2. The addition of Fe onto the Mn/TiO_2 catalyst improves the NOx removal activity by NH_3 in a wide operating temperature window, including the low temperature region less than 250 °C, regardless of the catalyst preparation methods. Including NO_2 ($NO_2/NO = 1$) in the feed gas stream further enhances the low temperature deNOx activity of $Mn/Fe/TiO_2$ catalyst.

1. Introduction

With its high fuel efficiency and relatively low emission of CO_2, the diesel engine has been widely employed in next-generation vehicles [1]. CO and HCs (hydrocarbons) may be readily oxidized by diesel oxidation catalyst (DOC) under the oxygen-rich diesel exhaust gas condition [2]. The emission of NOx then becomes a primary concern among the air pollutants from the engine [3]. Selective catalyst reduction (SCR) of NOx by urea is one of the most promising technologies to meet the stringent worldwide emission regulations, including EURO V and SULEV. CuZSM5, FeZSM5 and V_2O_5–WO_3/TiO_2 catalysts have been recognized as commercial catalysts for the urea-SCR technology [4–7]. However, they still suffer from their weak low temperature activity and the public perception of the catalyst composition, mainly copper and vanadium employed for the catalytic system [8,9]. The exhaust gas temperature from a diesel engine, light (150–250 °C) and heavy duty (200–350 °C), is significantly lower than that from a gasoline engine [10].

Mn-based catalysts including MnOx [11], MnOx–CeO_2 [12], Mn/TiO_2 [13], Mn–Fe/TiO_2 [14], Mn–Ce/USY [15], Mn–Fe/MPS [16] and Mn/Al-SBA-15 [17] have been proposed as eco-friendly low temperature SCR catalysts, especially for stationary sources. It should be noted that Mn is generally recognized as a less toxic metal component compared to Cu, V, Ni, and Co commonly employed for the preparation of SCR catalyst [18]. Recently, Wu et al. reported the high deNOx activity of Mn/TiO_2 catalyst prepared by sol–gel method at the reaction temperature of 100 °C [19]. In addition, Li et al. reported the improvement of deNOx performance over Mn/TiO_2 catalyst upon the replacement of the Mn precursor from nitrate to acetate to improve the dispersion of MnOx during the catalyst preparation procedure [20]. However, the deNOx catalytic performance of the Mn-based catalysts reported so far was generally examined at relatively lower reactor space velocity (8000–30,000 h^{-1}) and narrow temperature range (<250 °C) without H_2O in feed. Due to the dynamic operation of a diesel engine under excess lean air condition, an SCR activity test for developing a commercial urea-SCR catalyst should be conducted under a variety of the reactor operating conditions, including high reactor space velocity and wider temperature window [21,22]. In addition, the effect of water included in the exhaust gas stream from the engine on the NO removal activity of SCR catalyst can never be ignored, since the exhaust gas certainly contains H_2O in a range of the content, 10% [23,24].

The deNOx activity of Mn/TiO_2 catalysts varies with respect to their preparation method, particularly sol–gel and impregnation, regardless of Mn loading [25–27], primarily due to the unique structure and phase of MnOx formed onto or into TiO_2. However, a systematic or direct comparative study for the deNOx activity of Mn/TiO_2-based catalyst with respect to the preparation method including sol–gel and impregnation has been rarely reported, although it was recognized as an excellent low temperature SCR catalyst by Smirniotis et al. [13].

The purpose of the present study is to elucidate the unique features of the deNOx performance and catalytic properties of the s-Mn/TiO_2 and i-Mn/TiO_2 prepared by sol–gel and impregna-

* Corresponding author. Tel.: +82 54 279 2264; fax: +82 54 279 8299.
E-mail address: isnam@postech.ac.kr (I.-S. Nam).

0920-5861/$ – see front matter © 2010 Elsevier B.V. All rights reserved.
doi:10.1016/j.cattod.2010.02.074

tion (incipient wetness) methods, respectively, under realistic SCR reactor operating conditions anticipated for the after-treatment system of a diesel engine. The effect of Mn loadings on the deNOx performance of Mn-based catalysts was examined within a wide operating temperature window (100–400 °C) at relatively higher reactor space velocity (100,000 h^{-1}) under a feed gas composition including 10% H_2O. The deNOx performance and characteristics of s-Mn/TiO_2 catalyst were systematically determined by directly comparing the SCR activity of i-Mn/TiO_2 with respect to their Mn content. In addition, the role of Fe as an additive to the Mn/TiO_2 catalyst for the SCR activity was also investigated. Finally, NO_2 was included in the feed gas stream to further enhance the NOx removal activity of the Mn/Fe/TiO_2 catalyst, particularly in the low temperature range of less than 200 °C.

2. Experimental

2.1. Catalyst preparation

Mn/TiO_2 and Mn/Fe/TiO_2 catalysts were prepared by two typical preparation methods, one-step sol–gel [19] and incipient wetness methods [14]. To prepare s-Mn/TiO_2 and s-Mn/Fe/TiO_2 catalysts by sol–gel method, ample amounts of $Mn(NO_3)_2$ and $Fe(NO_3)_2$ were dissolved in H_2O and acetic acid. The solution was slowly added by buret into $Ti(OC_4H_9)_4$ dissolved in ethanol, and mixed intensively for 1 h. The solution underwent vigorous mixing again for another 24 h and then aged for an additional 72 h. The formed gel was oven-dried at 110 °C for 12 h, followed by calcination in air at 500 °C for 5 h.

For i-Mn/TiO_2 and i-Mn/Fe/TiO_2 prepared by incipient wetness method, commercial TiO_2 (Hombikat) was impregnated by the Mn and Fe nitrate solutions to fill up the pore volume of the TiO_2, catalyst support. The catalysts were then dried at 110 °C for 12 h in an oven. The samples were then calcined at 500 °C for 5 h in air flow. In addition, i-Mn/s-TiO_2 catalyst was prepared by impregnating $Mn(NO_3)_2$ onto s-TiO_2 by sol–gel method for a comparative study.

2.2. Catalyst characterization

BET surface areas of the catalysts were measured with a sorption analyzer (Micromeritics ASAP-2010) using liquid nitrogen at −196 °C. The catalysts were pretreated at 200 °C for 5 h under vacuum condition before measurement. To examine X-ray diffraction (XRD) spectra of the catalysts prepared in the present study, an XPERT PRO MPD X-ray diffractometer (PANalytical) was employed. Cu $K_{\alpha-1}$ (λ = 0.15406 nm) was used as a radiation source and the spectra were collected in the region of 2θ = 10–70° at 40 kV and 30 mA of X-ray gun. The XRD peaks were identified by using JCPDS data files.

The field emission-high resolution transmission electron microscopy (FE-HRTEM) images of the catalysts employed were obtained over a JEM 2100F instrument (JEOL) operated at 200 kV. The catalyst sample for TEM study was prepared by dispersing it with ethanol, dropping onto a holly carbon film supported on a copper grid and finally drying in an oven (110 °C).

2.3. Reaction system

A catalytic activity test using 1 g of the catalyst (20/30 mesh) was carried out in aluminum tube reactor (3/8 inch i.d.). A detailed flow diagram of the reactor system can be observed elsewhere [28]. The typical feed gas condition includes 500 ppm NOx (500 ppm NO or 250 ppm for both NO and NO_2), 500 ppm NH_3, 5% O_2, 10% H_2O and N_2 balance. Note that NH_3 was employed as a reductant in the present study for experimental convenience, since urea can be easily decomposed to NH_3 on the catalyst surface [29]. The inlet and outlet concentrations of NO, NO_2 and NH_3 were determined by on-line chemiluminescence NO–NOx analyzer (Thermo Environmental Instrument, Model 42C) and FT-IR (Nicolet 5700, Thermo Electron Co.) equipped with a gas-cell. The reactor space velocity (SV) for the catalyst activity test was typically 100,000 h^{-1}. Prior to each activity test, all the catalysts charged into the reactor were pretreated at 500 °C for 1.5 h in air flow.

3. Results and discussion

3.1. Effect of Mn contents on deNOx activity of Mn/TiO_2-based catalysts

Fig. 1 shows the deNOx activity over s-Mn/TiO_2, i-Mn/TiO_2 and i-Mn/s-TiO_2 catalysts with respect to their Mn content. When the Mn loaded onto the catalyst increases from 13 to 30 wt.%, the deNOx performance over s-Mn/TiO_2 catalyst is significantly enhanced. However, the catalytic activity over i-Mn/TiO_2 catalyst decreases as the content of Mn is increased from 13 to 28 wt.%. At 250 °C, 90% of the NO conversion has been achieved over s-Mn(30 wt.%)/TiO_2, while 65% is observed over i-Mn(13 wt.%)/TiO_2. The deNOx activity of i-Mn/s-TiO_2 catalysts, however, is in the range of that over i-Mn/TiO_2 catalysts. These results simply indicate that the SCR performance and physicochemical characteristics of Mn/TiO_2 catalysts vary with respect to the method of the catalyst preparation. Wu et al. reported that the deNOx activity of Mn/TiO_2 catalysts was similar, regardless of the preparation method (sol–gel and impregnation) and their Mn content [30]. It may be probably due to the differences in the preparation procedure of the catalysts and the reaction condition employed, particularly water in the feed gas stream and the reactor space velocity.

As the amounts of Mn loaded onto i-Mn/TiO_2 and i-Mn/s-TiO_2 catalysts increased, the BET surface area of the catalysts was decreased, as listed in Table 1, regardless of TiO_2, Hombikat and

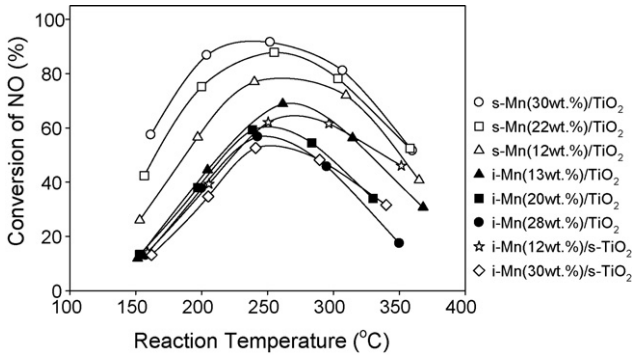

Fig. 1. DeNOx activity of the Mn/TiO_2 catalysts with respect to the Mn contents and preparation method. Feed gas composition: 500 ppm NO, 500 ppm NH_3, 5% O_2, 10% H_2O, and balance N_2; catalyst: 1 g; SV: 100,000 h^{-1}.

Table 1
BET surface area of the catalysts.

Catalysts	BET surface area (m^2/g)
s-TiO_2	110
s-Mn(12 wt.%)/TiO_2	125
s-Mn(22 wt.%)/TiO_2	130
s-Mn(30 wt.%)/TiO_2	123
TiO_2 (hombikat)	338
i-Mn(13 wt.%)/TiO_2	110
i-Mn(20 wt.%)/TiO_2	92
i-Mn(28 wt.%)/TiO_2	78
i-Mn(12 wt.%)/s-TiO_2	97
i-Mn(30 wt.%)/s-TiO_2	68

sol–gel prepared. It may be probably caused by filling and plugging the pores of the supports by Mn during the course of the impregnation procedure [31]. However, the BET surface area of s-Mn/TiO_2 catalysts even slightly increases as the Mn content of the catalyst increases. No pore plugging or filling of s-Mn/TiO_2 may be anticipated, since Mn has been incorporated into the infra-structure of TiO_2 during the one-step sol–gel synthesis of the catalyst [27]. Furthermore, the increase of the surface area of s-Mn/TiO_2 is mainly attributed to the incorporation of Mn ions into TiO_2 structure, providing additional nucleation sites and/or moderating the sintering of TiO_2 during the calcination procedure of the catalysts prepared [27,32,33].

3.2. State of Mn on the surface of Mn/TiO_2-based catalysts

3.2.1. XRD

To obtain structural information of the Mn included in the Mn/TiO_2 catalysts prepared by sol–gel and impregnation methods, XRD patterns of the catalysts were examined as shown in Fig. 2. A variety of the XRD peaks to be assigned to MnO_2 are observed over i-Mn/TiO_2, revealing that the crystalline MnO_2 exists on the catalyst surface. As the content of Mn for i-Mn/TiO_2 increases, the XRD peaks attributed to MnO_2 become apparent. However, s-Mn/TiO_2 catalyst shows weaker XRD peak intensity of MnO_2 than i-Mn/TiO_2. Especially, no peak for the formation of MnO_2 is observed over the catalysts containing Mn content less than 30 wt.%. It may be due to the fact that Mn is well incorporated into the matrix of TiO_2 [34] and/or MnO_2 is existing in an amorphous or highly dispersed phase on the catalyst surface [19,33]. In addition, the width of the XRD peaks typical for TiO_2 over s-Mn/TiO_2 catalyst is broader than that over i-Mn/TiO_2. It simply reveals that the matrix of the TiO_2 structure has been altered by Mn during the course of the sol–gel preparation of the catalyst [27].

To further discriminate the state of Mn included in the Mn/TiO_2 catalysts prepared by sol–gel and impregnation methods, a peak shift of the XRD patterns in the range of 2θ from 35 to 40° for TiO_2 has been specifically examined as shown in the inset of Fig. 2. s-TiO_2 prepared by sol–gel method reveals a peak at 37.85° assigned to the (0 0 4) plane of TiO_2 (anatase) as shown in Fig. 2(a). As the content of Mn included in s-TiO_2 increases, the peak attributed to TiO_2 shifts to the higher range of 2θ, 38.05° for s-Mn(12 wt.%)/TiO_2, 38.35° for s-Mn(22 wt.%)/TiO_2 and 38.39° for s-Mn(30 wt.%)/TiO_2 as shown in Fig. 2(c)–(e). However, a peak shift over i-Mn/TiO_2 is hardly observed within the 2θ range from 37.95° for TiO_2 (Hombikat) to 37.97° for i-Mn(28 wt.%)/TiO_2 as shown in Fig. 2(f)–(i). In addition, no peak shift of TiO_2 over i-Mn(30 wt.%)/s-TiO_2 at 37.88° from that of s-TiO_2 at 37.85° has been basically observed, as shown in Fig. 2(a) and (b). This result may simply indicate again that Mn is well incorporated into the structural matrix of TiO_2 during the preparation of s-Mn/TiO_2 by sol–gel method.

Table 2
d_{004} of TiO_2 obtained from XRD result.

Catalyst	d (Å)
s-TiO_2	2.375
s-Mn(12 wt.%)/TiO_2	2.363
s-Mn(22 wt.%)/TiO_2	2.345
s-Mn(30 wt.%)/TiO_2	2.342
TiO_2 (hombikat)	2.369
i-Mn(28 wt.%)/TiO_2	2.368
i-Mn(30 wt.%)/s-TiO_2	2.373

Since the Mn^{4+} ion incorporated into the lattice of TiO_2 may replace Ti^{4+} ion included in s-Mn/TiO_2 during the sol–gel procedure, the lattice space of the (0 0 4) plane of TiO_2 decreases with respect to the catalyst Mn content as listed in Table 2, mainly due to the difference in the atomic radius of Mn^{4+} (0.60 Å) and Ti^{4+} (0.68 Å) [24,32,34]. The Mn incorporated into the matrix of TiO_2 will also improve the dispersion of Mn on the surface of TiO_2. It plays an important role for reducing NO by NH_3, although Wu et al. insisted that the dispersion of Mn was increased simply due to the formation of amorphous MnO_2 on the surface of Mn/TiO_2 prepared by sol–gel method [19,30]. In contrast, the lattice space of the (0 0 4) plane over the i-Mn/TiO_2 catalyst hardly decreases compared to that over TiO_2 (Hombikat), although 28 wt.% of Mn was loaded onto the catalyst. The lattice distance over i-(30 wt.%)/s-TiO_2 catalyst is similar to that over s-TiO_2 as clearly listed in Table 2. Mn included in i-Mn/TiO_2 and i-Mn/s-TiO_2 catalysts prepared by the impregnation method may not be incorporated into the matrix of TiO_2, but simply exists on the surface of TiO_2 resulting in the poor dispersion of MnO_2, regardless of TiO_2 supports, Hombikat and sol–gel prepared.

On the other hand, the decreasing degree of the lattice space is markedly moderated when the Mn content of the catalyst reaches 30 wt.%. In addition, an XRD peak assigned to MnO_2 starts to appear over s-Mn(30 wt.%)/TiO_2 catalyst as shown in Fig. 2(e). The Mn content of 22 wt.% may be the highest capacity of Mn to be incorporated into the matrix of TiO_2. Although all of Mn over s-Mn(30 wt.%)/TiO_2 catalyst could not be incorporated into the lattice of TiO_2, the rest of the MnO_2 may exist on the catalyst surface and become an additional reaction site for the present SCR reaction [13,14]. It may be also reflected by the decreasing trend of the BET surface area

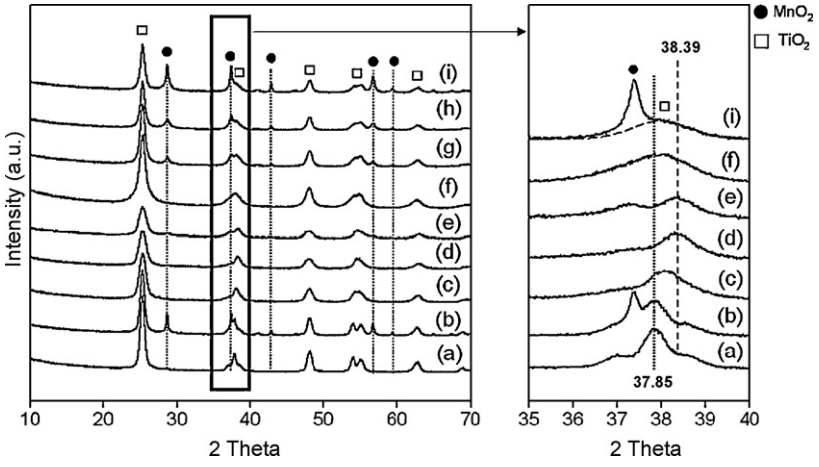

Fig. 2. XRD patterns of TiO_2 and Mn/TiO_2 catalysts. (a) s-TiO_2, (b) i-Mn(30 wt.%)/s-TiO_2, (c) s-Mn(12 wt.%)/TiO_2, (d) s-Mn(22 wt.%)/TiO_2, (e) s-Mn(30 wt.%)/TiO_2, (f) TiO_2 (hombikat), (g) i-Mn(13 wt.%)/TiO_2, (h) i-Mn(20 wt.%)/TiO_2, and (i) i-Mn(28 wt.%)/TiO_2.

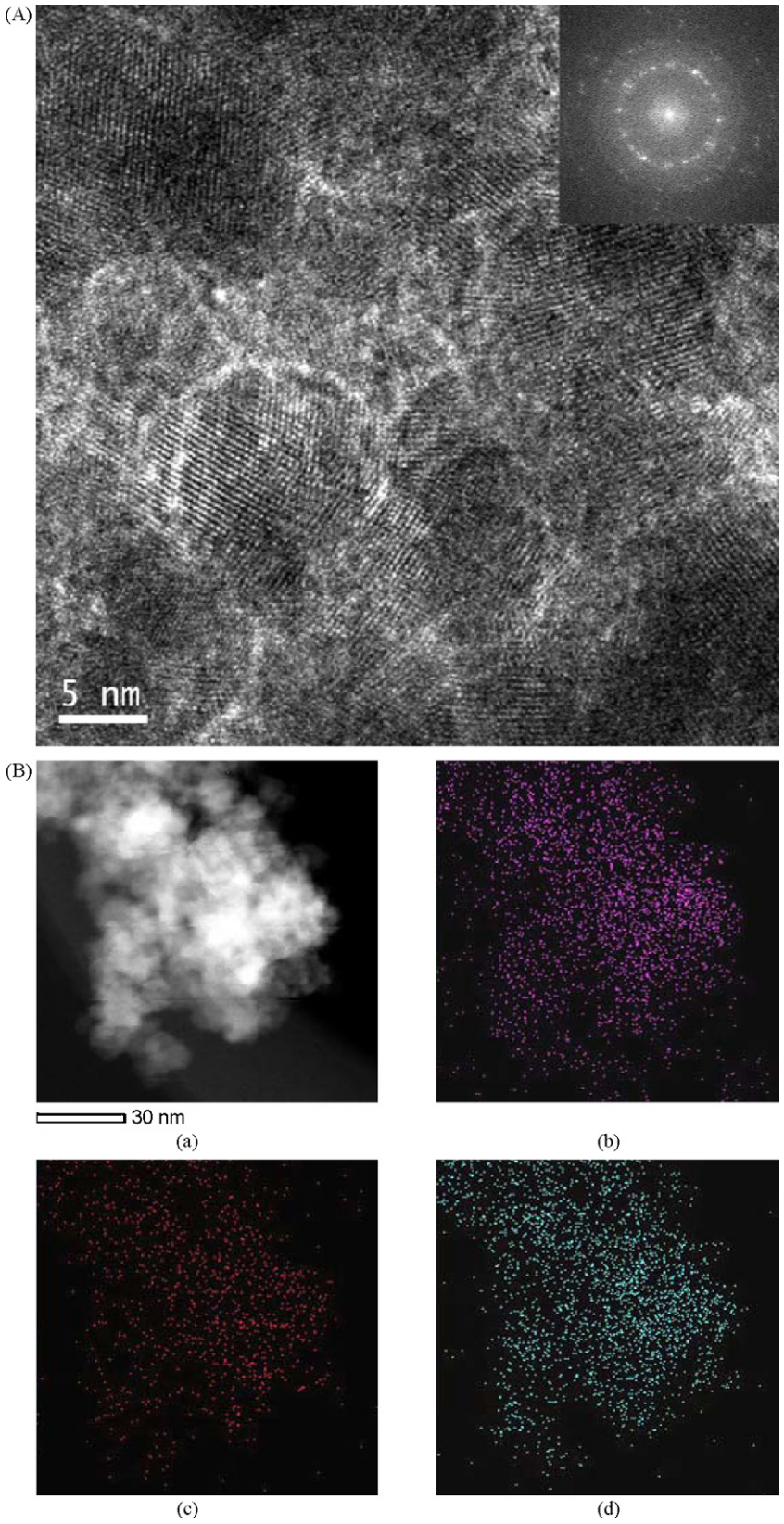

Fig. 3. HRTEM image for SAED patterns (A) and EDS mapping (B) of the s-Mn(22 wt.%)/TiO_2 catalyst. (a) STEM image, (b) O, (c) Ti, and (d) Mn.

of s-Mn(30 wt.%)/TiO_2 (123 m^2/g) from that of s-Mn(22 wt.%)/TiO_2 (130 m^2/g). The additional Mn may block and fill the pore network of TiO_2 as observed by the change of the surface area of i-Mn/TiO_2 listed in Table 1.

3.2.2. TEM image and EDS mapping

TEM images and SAED (selected area electron diffraction) patterns of s-Mn(22 wt.%)/TiO_2 and i-Mn(20 wt.%)/TiO_2 catalysts were examined to ensure the incorporation of Mn into the structural

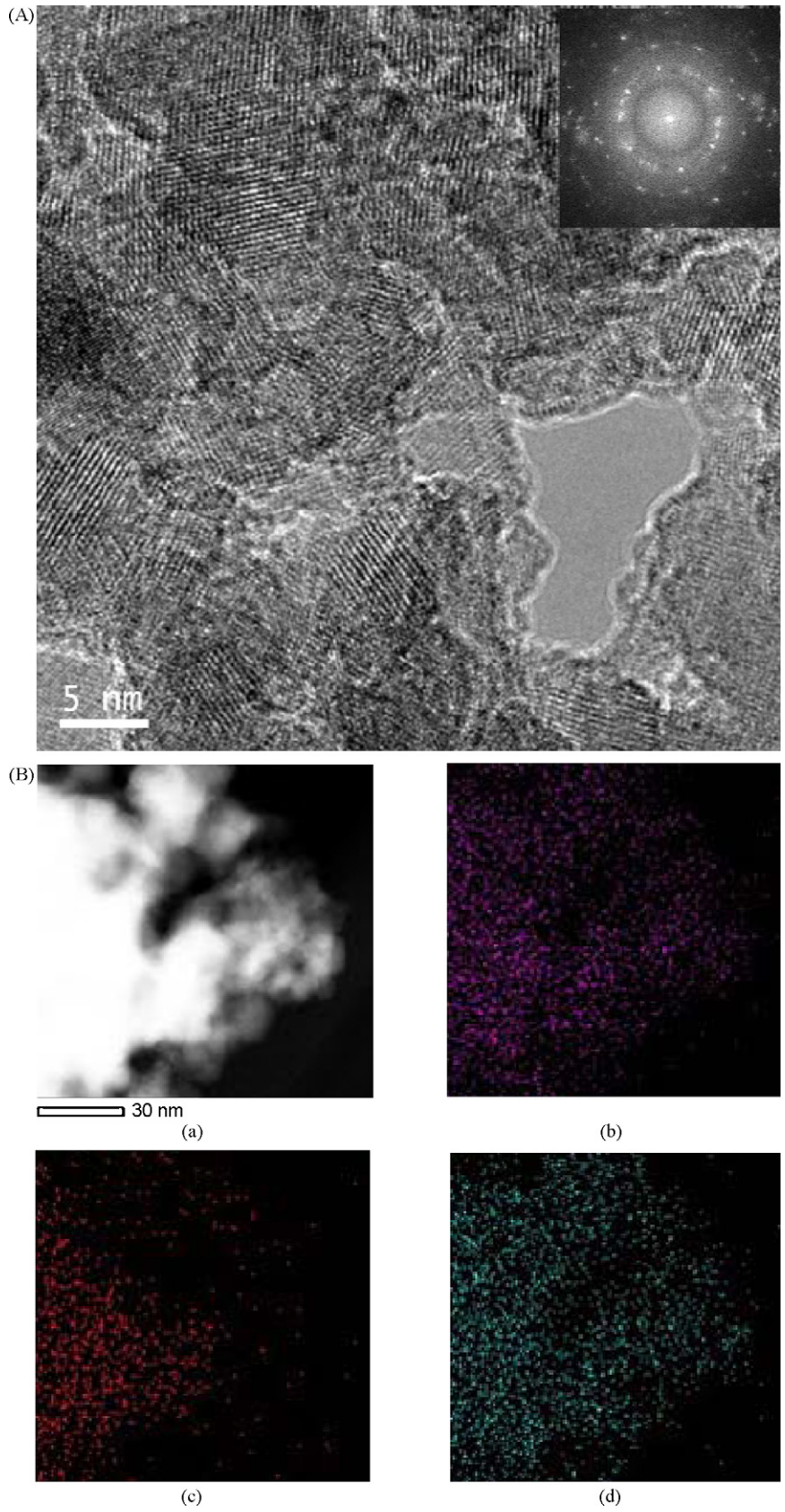

Fig. 4. HRTEM image for SAED patterns (A) and EDS mapping (B) of the i-Mn(20 wt.%)/TiO_2 catalyst. (a) STEM image, (b) O, (c) Ti, and (d) Mn.

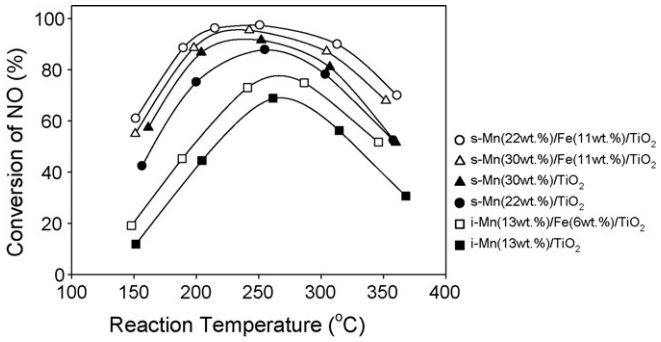

Fig. 5. Effect of Fe on deNOx performance over Mn/TiO_2 catalysts. Feed gas composition: 500 ppm NO, 500 ppm NH_3, 5% O_2, 10% H_2O, and balance N_2; catalyst: 1 g; SV: 100,000 h^{-1}.

matrix of TiO_2. The crystallization of Mn over i-Mn/TiO_2 seems to be more apparent than that over s-Mn/TiO_2 as contrasted in Figs. 3 and 4A, which was also anticipated by their XRD patterns discussed with Fig. 2. Both Mn and Ti distributions along with O on the surface of s-Mn/TiO_2 are nearly identical to the EDS mapping results shown in Figs. 3B (c) and (d). Mn also exists where Ti does. However, both distributions over i-Mn/TiO_2 are distinct as shown in Figs. 4B (c) and (d). Both metals may be hardly incorporated in each other. Note that the distribution of O over i-Mn/TiO_2 is similar to that of Mn.

Since Mn over s-Mn/TiO_2 catalyst is well incorporated into the lattice of TiO_2 as clearly determined by XRD, a similar distribution of both Mn and Ti can be readily anticipated. However, Mn is aggregated in the form of crystalline MnO_2 over i-Mn/TiO_2 as discussed and no correlation of the distributions of Mn and Ti can be determined by the EDS mapping result. The higher dispersion of Mn on the surface of s-Mn/TiO_2 than that of i-Mn/TiO_2 catalyst may indicate the high deNOx performance of s-Mn/TiO_2 catalyst [14,15,19].

3.3. Effect of Fe on the deNOx activity of Mn/TiO_2 catalyst

To enhance the low temperature SCR activity of the Mn/TiO_2 catalyst, Fe, a catalyst promoter was added onto the catalyst surface. Upon the addition of Fe onto the s-Mn/TiO_2 and i-Mn/TiO_2 catalysts, the deNOx performance and the operation temperature window were apparently enhanced and widened as shown in Fig. 5. Mn and Fe were simultaneously added into the $Ti(OC_4H_9)_4$ dissolved in ethanol for the preparation of s-$Mn/Fe/TiO_2$ by sol–gel method. As the content of Fe increased up to 11 wt.%, the deNOx activity over the s-$Mn/Fe/TiO_2$ catalyst was enhanced. However, when the Fe content was higher than 11 wt.%, the gel of $Mn/Fe/TiO_2$ catalyst was hardly formed during the sol–gel procedure.

Upon the addition of Fe to both types of Mn/TiO_2 catalysts, the XRD peak intensity of MnO_2 becomes weaker as shown in Fig. 6. MnO_2 may then exist in a less crystallized form and the metal dispersion on the catalyst surface will be improved [14]. Fe over s-$Mn/Fe/TiO_2$ catalyst may moderate the sintering of TiO_2 expected during the course of the catalyst calcination procedure at 500 °C for 5 h [19]. The width of the peaks to be assigned to TiO_2 becomes broader [19]. Qi et al. reported that the strong interaction of manganese to iron oxides might improve the dispersion of Mn on the surface of i-$Mn/Fe/TiO_2$ catalyst [14]. Wu et al. also claimed that the interaction of the solid solution of manganese and iron oxides, formed on the surface of s-$Mn/Fe/TiO_2$ catalyst during the catalyst calcination procedure at 500 °C, prevented the catalyst from sintering and enhanced the Mn dispersion to achieve the high deNOx performance [19]. Fe added into Mn/TiO_2-based catalyst plays a role in improving the dispersion of MnO_2, recognized as one of the

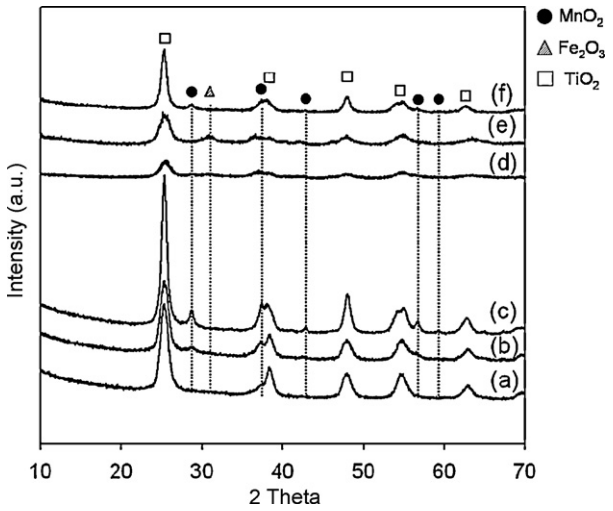

Fig. 6. XRD patterns for Mn/TiO_2 and $Mn/Fe/TiO_2$ catalysts. (a) s-Mn(22 wt.%)/TiO_2, (b) s-Mn(30 wt.%)/TiO_2, (c) i-Mn(13 wt.%)/TiO_2, (d) s-Mn(22 wt.%)/Fe(11 wt.%)/TiO_2, (e) s-Mn(30 wt.%)/Fe(11 wt.%)/TiO_2, and (f) i-Mn(13 wt.%)/Fe(6 wt.%)/TiO_2.

important catalyst characteristics for the present reaction system, regardless of the catalyst preparation methods.

On the other hand, the deNOx activity of s-Mn(22 wt.%)/Fe(11 wt.%)/TiO_2 catalyst is higher than that of s-Mn(30 wt.%)/Fe(11 wt.%)/TiO_2, while s-Mn(30 wt.%)/TiO_2 catalyst showed superior SCR performance to s-Mn(22 wt.%)/TiO_2 as shown in Fig. 5. Wang et al. reported that crystalline Fe_2O_3 started to form on the catalyst surface when the content of Fe on s-Fe/TiO_2 was higher than 20 wt.% [34]. The formation of the crystalline Fe_2O_3 over s-Mn(30 wt.%)/Fe(11 wt.%)/TiO_2 is clearly observed in Fig. 6(e). There may be a capacity for incorporating Mn and Fe into the matrix of Ti over s-$Mn/Fe/TiO_2$ by sol–gel method as discussed. The relatively higher deNOx activity over s-Mn(22 wt.%)/Fe(11 wt.%)/TiO_2 may then be understood.

3.4. Role of NO_2 included in feed gas stream

The role of the diesel oxidation catalyst (DOC) placed before the SCR reaction system installed into the commercial diesel aftertreatment system is to oxidize NO emitted from the engine to NO_2 [35,36]. It has been also commonly recognized that the addition of NO_2 into feed containing NO significantly improves the NO removal activity of an SCR catalyst [37]. Fig. 7 depicts the deNOx activity

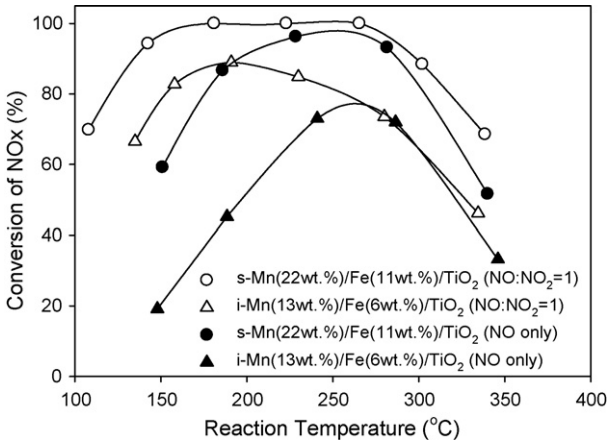

Fig. 7. Effect of NO_2 in the feed on deNOx performance of $Mn/Fe/TiO_2$ catalyst. Feed gas composition: 500 or 250 ppm NO, 500 ppm NH_3, 250 ppm NO_2, 5% O_2, 10% H_2O and balance N_2; catalyst: 1 g; SV: 100,000 h^{-1}.

over the Mn/Fe/TiO_2 catalysts with and without NO_2 in the feed stream.

When a 1:1 feed ratio of NO and NO_2 was maintained in the feed gas stream, the deNOx activity over the Mn/Fe/TiO_2 catalyst was drastically enhanced as shown in Fig. 7 [38]. The s-Mn(22 wt.%)/Fe(11 wt.%)/TiO_2 catalyst achieves nearly 100% of NOx conversion at 150 °C, when both NO and NO_2 are included into the feed. It may be mainly due to the fast SCR reaction of NO_2 compared to the standard SCR reaction of NO [39–42].

4. Conclusion

The deNOx activity of s-Mn/TiO_2 and i-Mn/TiO_2 catalysts prepared by sol–gel and impregnation methods has been examined. s-Mn/TiO_2 catalyst showed higher deNOx performance than i-Mn/TiO_2 catalyst in the reaction temperature window from 150 to 350 °C. The deNOx activity of s-Mn/TiO_2 catalyst was significantly enhanced as the content of Mn increased, whereas that of i-Mn/TiO_2 catalyst was decreased. The high deNOx performance of s-Mn/TiO_2 is mainly attributed to the high dispersion of MnO_2 on the catalyst surface by the well-incorporated Mn into the matrix of Ti during the sol–gel preparation of the catalyst. However, the crystalline form of MnO_2 was formed on the surface of i-Mn/TiO_2 prepared by the impregnation method. Upon the addition of Fe onto the Mn/TiO_2 catalyst, the SCR performance of the catalyst was improved. Also, the deNOx activity over Mn/Fe/TiO_2 catalyst was further enhanced, when both NO and NO_2 in a ratio of 1:1 were present in the feed gas stream. The commercial application of the Mn/TiO_2 catalyst prepared by sol–gel method as an environmentally friendly and low temperature SCR catalyst may be expected in the diesel after-treatment system including DOC.

Acknowledgments

This work was supported by the CEFV (Center for Environmentally Friendly Vehicle) of Eco-STAR project from MOE (Ministry of Environment, Republic of Korea) and the National Research Foundation of Korea (NRF) grant funded by the Korea government (MEST) (No. 20090092793).

References

[1] R.M. Heck, R.J. Farrauto, S.T. Gulati, Catalytic Air Pollution Control: Commercial Technology, second ed., John Wiley & Sons, Inc., 2002.
[2] F.C. Galisteo, R. Mariscala, M.L. Granados, J.L.G. Fierro, R.A. Daley, J.A. Anderson, Appl. Catal. B:Environ. 59 (2005) 227.
[3] W.S. Epling, L.E. Campbell, A. Yezerets, N.W. Currier, J.E. Parks I.I., Catal. Rev. 46 (2004) 164.
[4] A. Grossale, I. Nova, E. Tronconi, J. Catal. 265 (2009) 141.
[5] J.H. Park, H.J. Park, J.H. Baik, I.-S. Nam, C.H. Shin, J.-H. Lee, B.K. Cho, S.H. Oh, J. Catal. 240 (2006) 47.
[6] M.L.M. de Oliveira, C.M. Silva, R. Moreno-Tost, T.L. Farias, A. Jimenez-López, E. Rodríguez- Castellón, Appl. Catal. B:Environ. 88 (2009) 420.
[7] O. Krocher, Stud. Surf. Sci. Catal. 171 (2007) 261.
[8] Y.-M. Kuo, J. Gitschier, S. Packman, Hum. Mol. Genet. 6 (1997) 1043.
[9] Y. Li, H. Cheng, D. Li, Y. Qin, Y. Xie, S. Wang, Chem. Commun. 12 (2008) 1470.
[10] R.G. Gonzales, "Diesel Exhaust Emission System Temperature Test", T&D Report 0851-1816P, SDTDC, U.S. Department of Agriculture, December (2008).
[11] M. Kang, E.D. Park, J.M. Kim, J.E. Yie, Appl. Catal. A: Gen. 327 (2007) 261.
[12] G. Qi, R.T. Yang, J. Catal. 217 (2003) 434.
[13] P.G. Smirniotis, D.A. Pena, B.S. Uphade, Angew. Chem. Int. 40 (2001) 2479.
[14] G. Qi, R.T. Yang, Appl. Catal. B:Environ. B 44 (2003) 217.
[15] G. Qi, R.T. Yang, R. Chang, Catal. Lett. 87 (2003) 67.
[16] J. Huang, Z. Tong, Y. Huang, J. Zhang, Appl. Catal. B:Environ. 78 (2008) 309.
[17] X. Liang, J. Li, Q. Lin, K. Sun, Catal. Commun. 8 (2007) 1901.
[18] Manganese from Wikipedia, the free encyclopedia, "http://en.wikipedia.org/wiki/Mn".
[19] Z. Wu, B. Jiang, Y. Liu, Appl. Catal. B:Environ. 79 (2008) 347.
[20] J. Li, J. Chen, R. Ke, C. Luo, J. Hao, Catal. Commun. 8 (2007) 1896.
[21] M. Koebel, M. Elsener, M. Kleemann, Catal. Today 59 (2000) 335.
[22] F. Klingstedt, K. Arve, K. Ernen, D.Y. Murzin, Acc. Chem. Res. 39 (2006) 273.
[23] Y.-K. Youn, J.W. Park, C.-I. Kwon, J.-H. Lee, G.-K. Yeo, Y.-S. You, SAE, 2006-01-1370 (2006).
[24] Z. Liu, S.I. Woo, Catal. Rev. 48 (2006) 43.
[25] G. Bai, X. Fan, H. Wang, J. Xu, F. He, H. Ning, Catal. Commun. 10 (2009) 2031.
[26] S. Schimpf, M. Lucas, C. Mohr, U. Rodemerck, A. Brückner, J. Radnik, H. Hofmeister, P. Claus, Catal. Today 72 (2002) 63.
[27] M.M. Mohamed, I. Othman, R.M. Mohamed, J. Photochem. Photobiol. A 191 (2007) 153.
[28] J.H. Baik, S.D. Yim, I.-S. Nam, Y.S. Mok, J.-H. Lee, B.K. Cho, S.H. Oh, Ind. Eng. Chem. Res. 45 (2006) 5258.
[29] S.D. Yim, S.J. Kim, J.H. Baik, I.-S. Nam, Y.S. Mok, J.-H. Lee, B.K. Cho, S.H. Oh, Ind. Eng. Chem. Res. 43 (2004) 4856.
[30] B. Jiang, Y. Liu, Z. Wu, J. Harzard. Mater. 162 (2009) 1249.
[31] S. Neaţu, V.I. Pârvulescu, G. Epure, N. Petrea, V. Somoghi, G. Ricchiardi, S. Bordiga, A. Zecchina, Appl. Catal. B:Environ. 91 (2009) 546.
[32] J. Villaseñor, P. Reyes, G. Pecchi, Catal. Today 76 (2002) 121.
[33] D.A. Pena, B.S. Uphade, P.G. Smirniotis, J. Catal. 221 (2004) 421.
[34] Y. Wang, H. Cheng, Y. Hao, J. Ma, W. Li, S. Cai, J. Mater. Sci. 34 (1999) 3721.
[35] T.J. Wang, S.W. Baek, J.-H. Lee, Ind. Eng. Chem. Res. 47 (2008) 2528.
[36] E. Xue, K. Seshan, J.R.H. Ross, Appl. Catal. B:Environ. 11 (1996) 65.
[37] M. Schwidder, S. Heikens, A.D. Toni, S. Geisler, M. Berndt, A. Brückner, W. Grünert, J. Catal. 259 (2008) 96.
[38] J.H. Baik, J.H. Rho, S.D. Yim, I.-S. Nam, J.-H. Lee, B.K. Cho, S.H. Oh, Stud. Surf. Sci. Catal. 159 (2006) 441.
[39] M. Koebel, G. Madia, F. Raimondi, A. Wokaun, J. Catal. 209 (2002) 159.
[40] C. Ciardelli, I. Nova, E. Tronconi, D. Chatterjee, T. Burkhardt, M. Weibel, Chem. Eng. Sci. 62 (2007) 5001.
[41] E. Tronconi, I. Nova, C. Ciardelli, D. Chatterjee, M. Weibel, J. Catal. 245 (2007) 1.
[42] M. Koebel, G. Madia, M. Elsener, Catal. Today 73 (2002) 239.